

## ABSTRACT

Development of optimal infrasound signal detection procedures needs to consider signal and noise characteristics as well as array configuration. We investigate the performance of automated infrasound detectors on impulsive and extended signals. In the first case, waveforms recorded by the Korean infrasound array CHNAR are analyzed using the progressive multi-channel correlation method (Cansi, 1995) and the adaptive F detector (Arrowsmith et al., 2009). The automated techniques are compared to the signals identified by five independent analysts. The effectiveness of the detectors are shown to be a function of array aperture, RMS amplitudes (1.2-4.5 mPa), and wind conditions. The detection probabilities (PD) are most strongly influenced by noise levels with an average PD of ~0.40 under low noise conditions (1.7 mPa) and an average of ~0.23 under high noise levels (2.9 mPa). In the second case, we design an automatic infrasound detector using single seismic stations in the western US to analyze the signal characteristics of known impulsive and extended signals. Based on the RMS amplitude measurement of pre-group velocity windows, arrival time, SNR, and the duration of the signal were estimated. We identify key features in establishing infrasound bulletins through detector tuning at a single array as well as the effective use of a network of sensors.

## Automatic Infrasound Detection using Infrasound Sensors

Two automated detectors, the progressive multi-channel correlation (PMCC) (Cansi, 1995) and adaptive F-detector in InfraMonitor (IM) (Arrowsmith et al., 2009), that rely on waveform correlation were used in this case. Both detectors were applied to a dataset recorded at the seismo-acoustic array, CHNAR, located within the continent of South Korea (Fig. 1). In the case of the adaptive F-detector where the C value characterizes the adaptation, the first two-hours of data have relatively high C values with low wind velocities, while the last two-hours of data have smaller C values with higher wind velocities (Fig. 2).

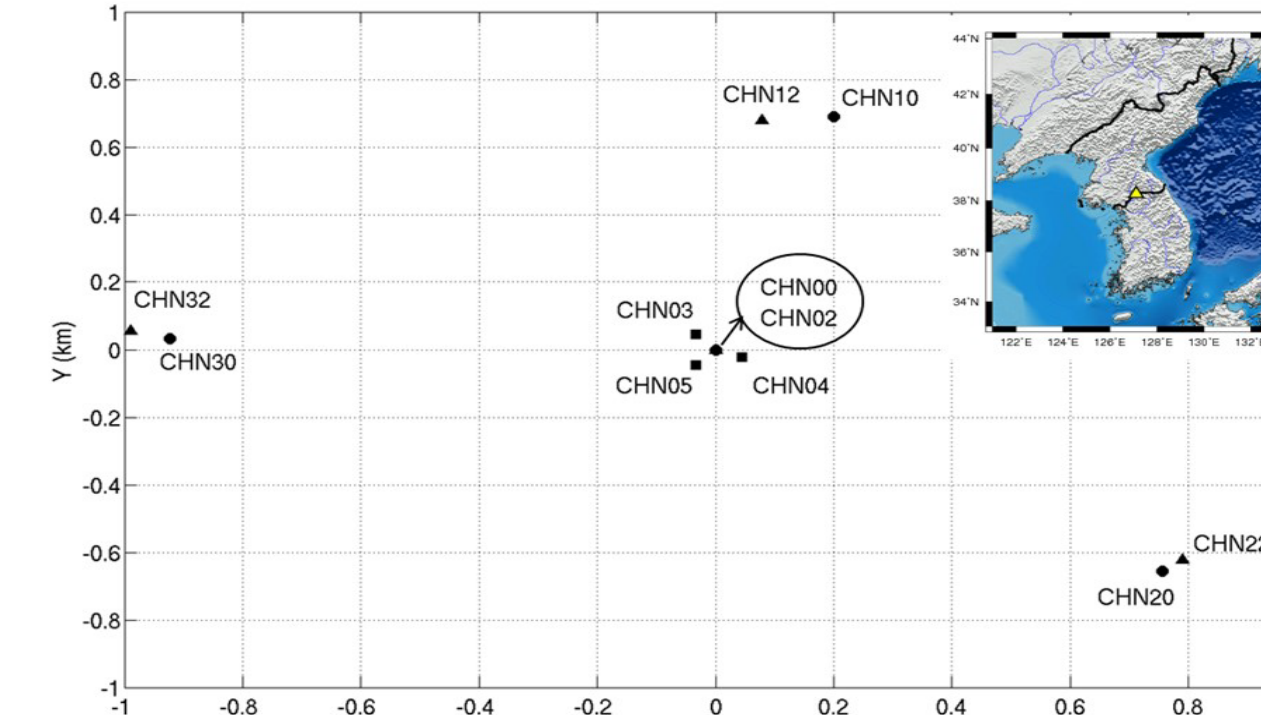


Figure 1. The physical configuration of CHNAR, consisting of a small (~100 m) infrasound array embedded in a larger (~1 km) array with sub-infrasound element.

PMCC and InfraMonitor (IM) were tested using four different starting configurations or sub-network. Both detectors use a time window of 20s with overlap of 50%. PMCC used consistencies of 0.1 and 0.5s with 4 threshold stations. For grouping into families, the standard deviation of 10° for azimuth and 20 m/s for phase velocity with a phase velocity range from 0.2 to 0.5 km/s were used. For IM,  $p$ -values of 0.01 and 0.05, and an adaptive window of 1 hour were used. Five analysts separately reviewed the same dataset used in the test of the automated systems and were free to define their own criteria for event identification.

In order to assess detector performance, Receiver Operating Characteristic curves (ROC) (Johnson and Dudgeon, 1993) were used to estimate the trade-off between the detection probability ( $PD = \text{number of detected signals/total number of signals}$ ) and the false-alarm probability ( $PF = \text{number of noise detections/total number of detections intervals during noise}$ ). Here, in the absence of ground truth, we use the *Estimated ROC* (EROC) where the total number of signals is defined by the analyst results (Fig. 3).

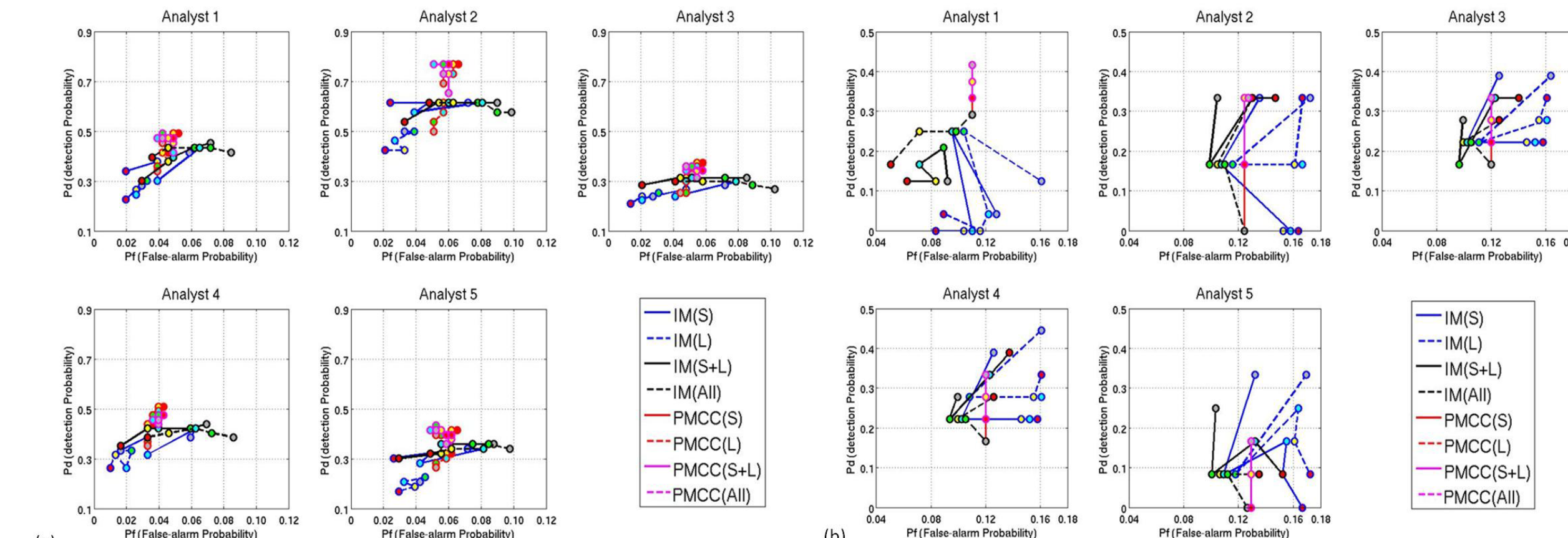


Figure 3. The EROC for the automatic detectors from (a) the first two-hours and (b) the last two-hours using data from the different aperture arrays. The warmer the color of the circles the smaller  $p$ -value for IM and the smaller consistency value for PMCC. The x-axes, false-alarm Probability, are exaggerated by a factor of (a) eight and (b) three.

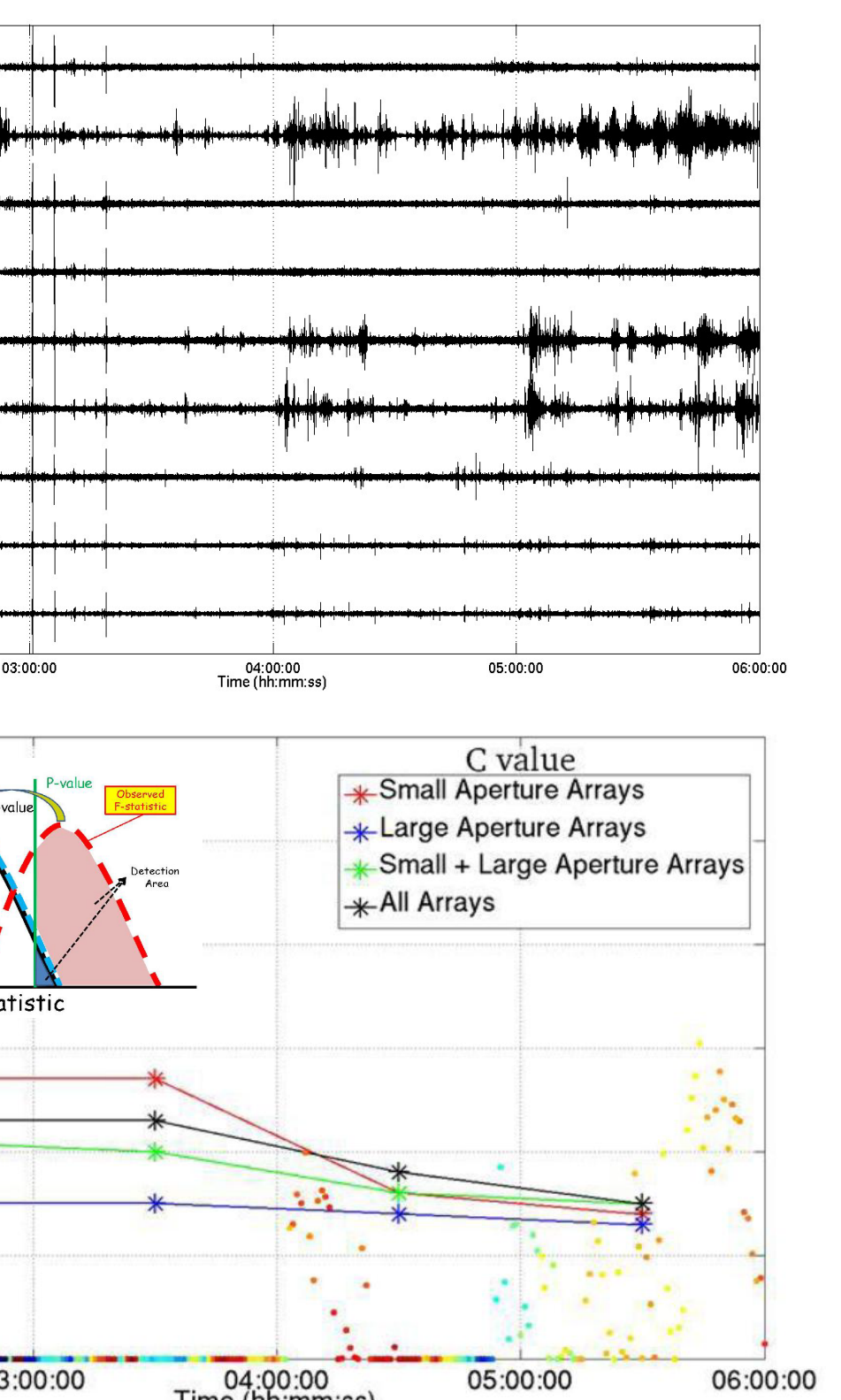


Figure 2. The 4-hour-dataset (02:00:00-06:00:00) in UTC, 11am-3pm in local time, Julian day 002, 2012) recorded at CHNAR (top). The relationship between the C value from InfraMonitor (diagram shown inside the bottom figure) and wind conditions with respect to different types of array apertures (bottom).

## Summary

- The first two hours of data produced higher detection probabilities and lower false alarm rates using both detectors relative to the second two hours of data.
- With the selected parameter ranges, PMCC produces higher detection probabilities (PD) than does IM during the first two hours while PMCC has slightly lower PD than IM in the last two hours.
- Both detection and false alarm rate increases with increasing  $p$ -value and decreasing consistency values.
- For both PMCC and IM, the use of combined small and large aperture arrays are recommended.
- The PD for both PMCC and IM are most strongly influenced by noise level, correlated with wind velocity, with an average PD of ~0.40 under low noise condition (1.7 mPa) and an average of ~0.23 under high noise level (2.9 mPa).

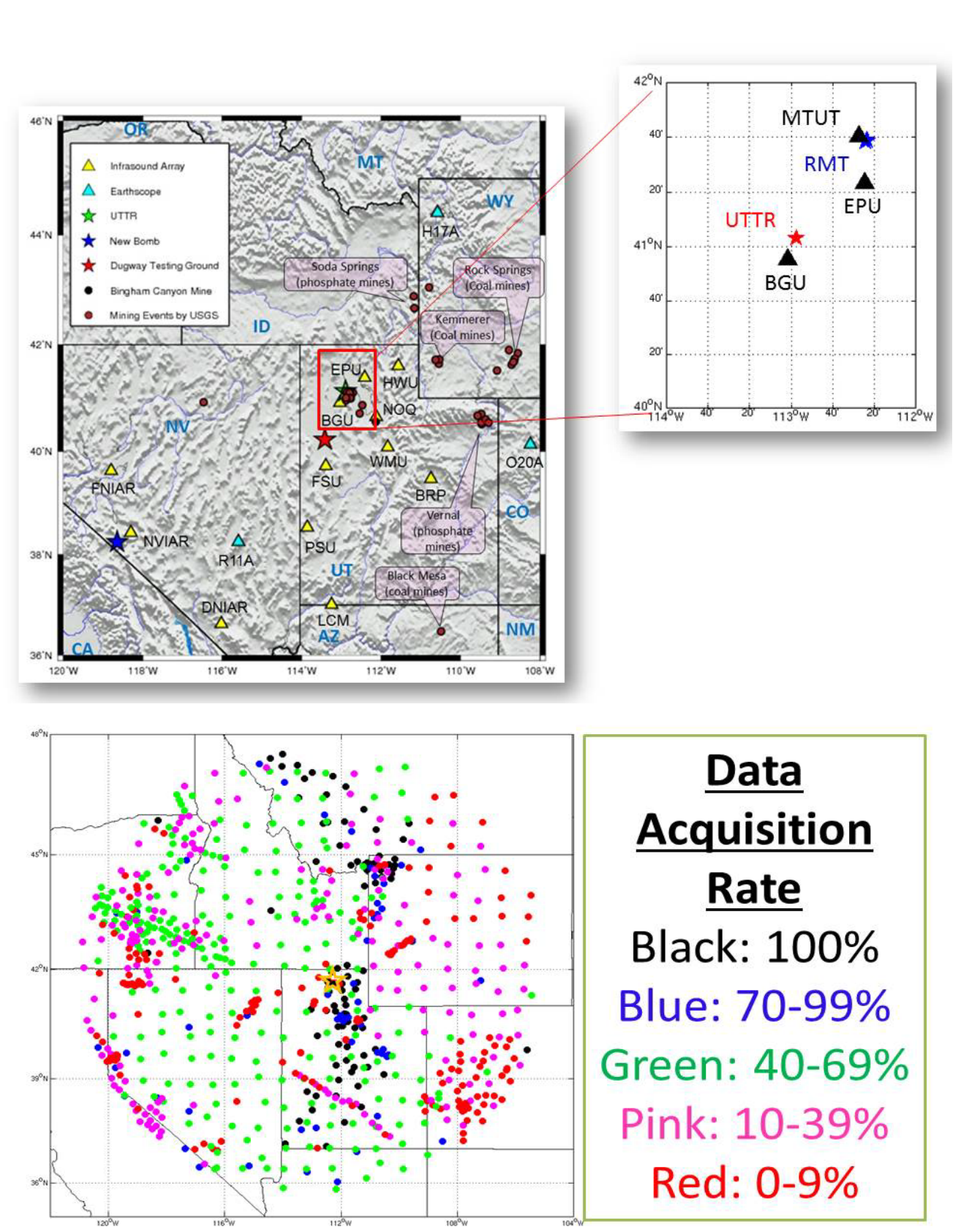
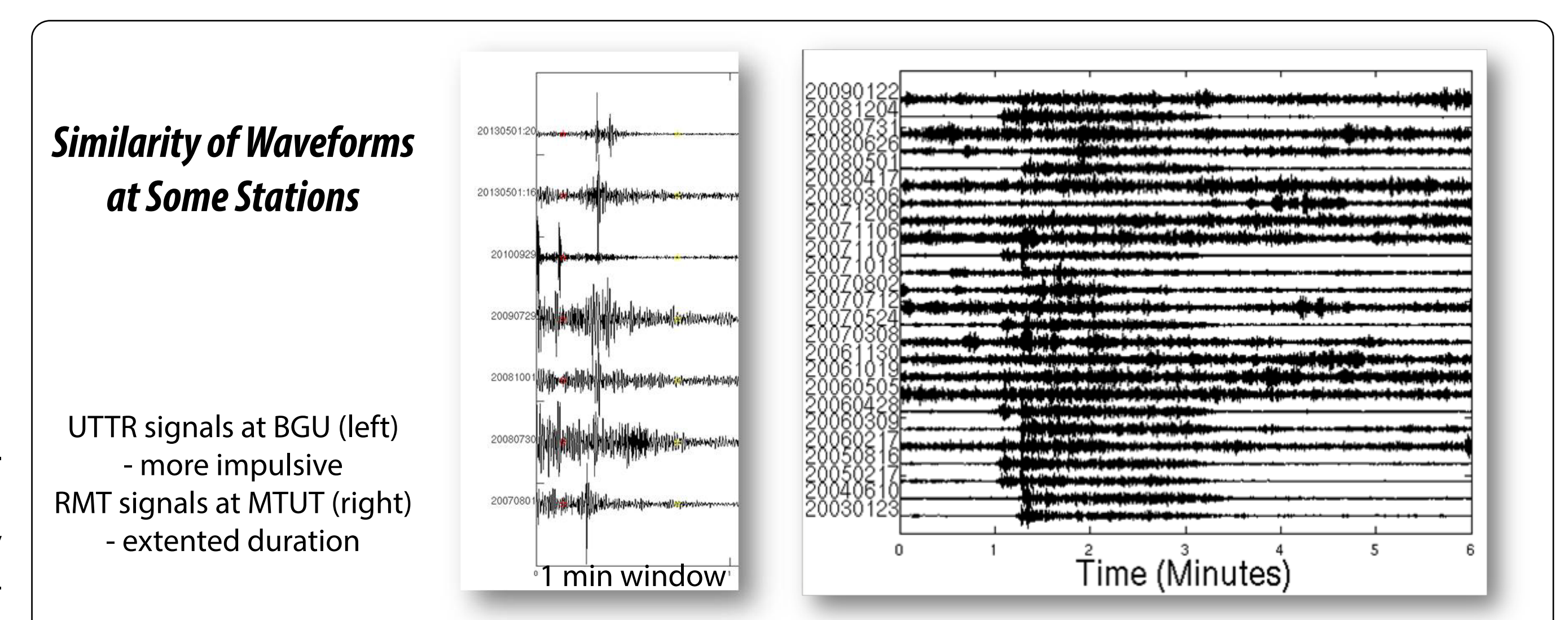


Figure 4. Top: Locations of known sources (Rocket Motor Test: RMT and Utah Test and Training Range: UTTR) and infrasound arrays in the study area. Bottom: seismic station map with data acquisition rate (by color) and source location (orange star).

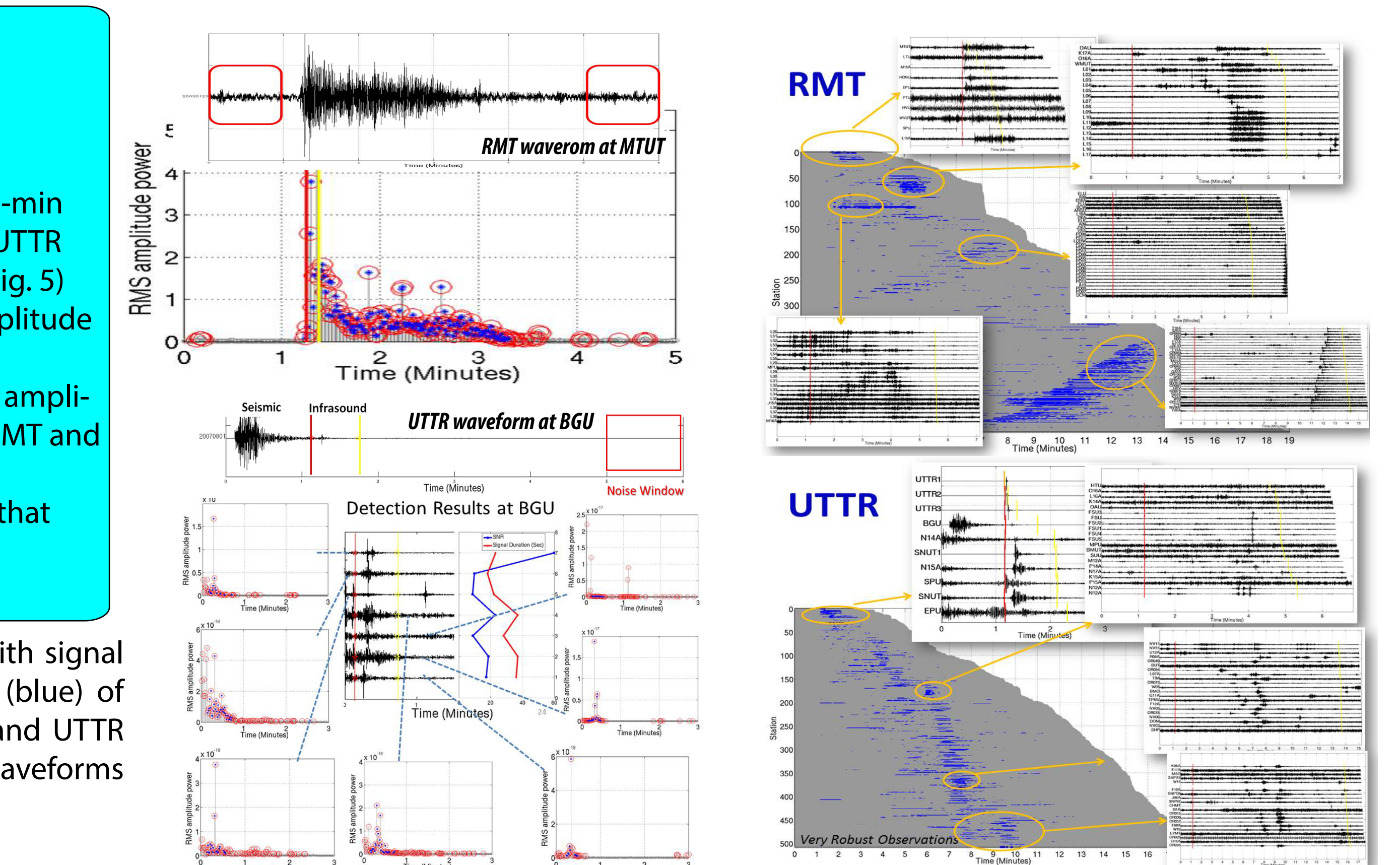
## Automatic Infrasound Detection using Single Seismic Stations

We utilize acoustic data recorded on single seismic stations including data from the USArray Transportable Array (TA) in addition to data from infrasound arrays in Utah and Nevada (Fig. 4) in this investigation. We explore the value of source ground truth information in enhancing signal detection procedures. Ground truth in this case consists of a total of 1116 stations were collected for the time period of the ground truth information. Stations have inhomogeneous data availability as function of time during this time period (Fig. 4, bottom).



Similarity of Waveforms at Some Stations

UTTR signals at BGU (left)  
- more impulsive  
RMT signals at MTUT (right)  
- extended duration



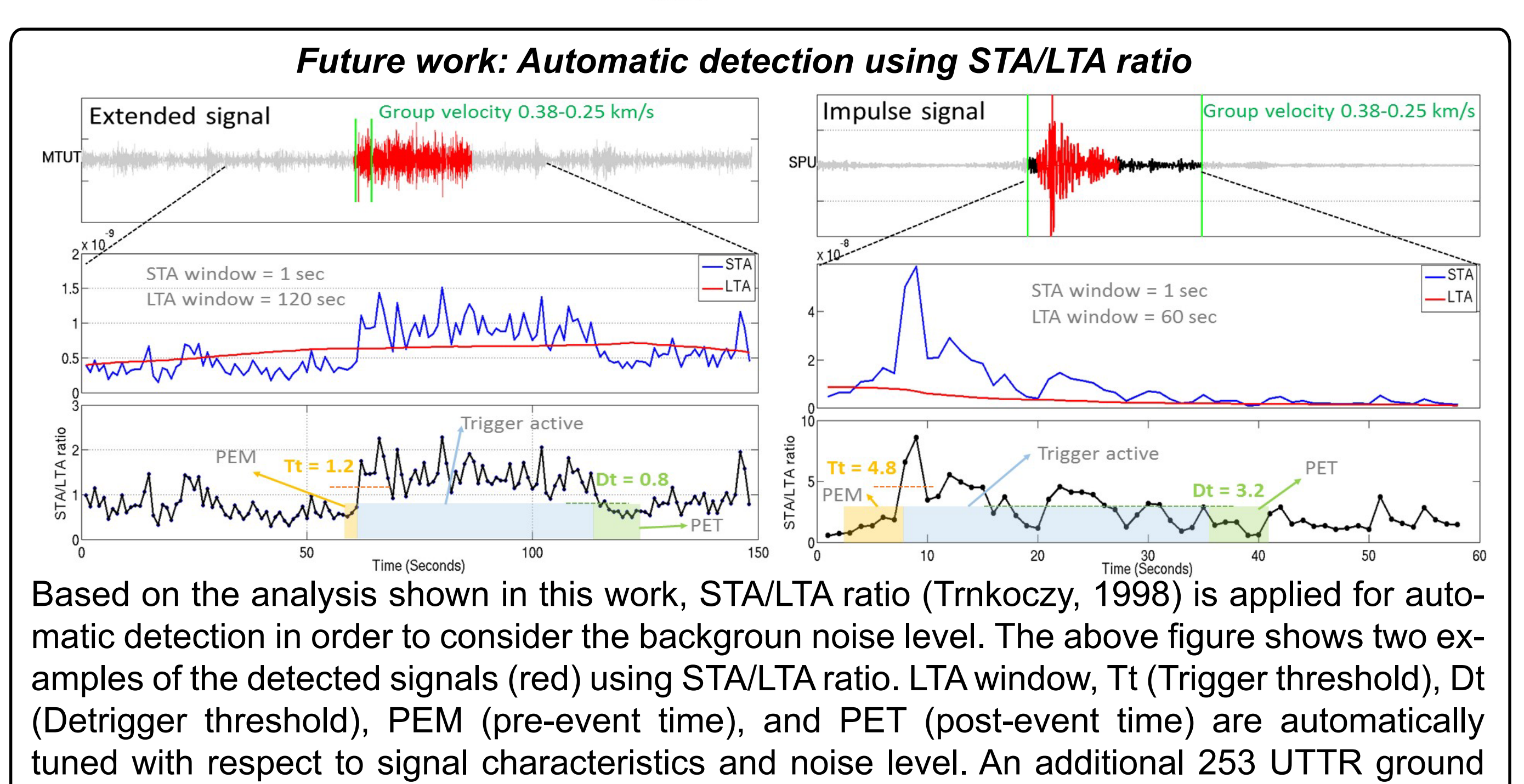
## Criteria for Automatic Signal Processing with Source Ground Truth

- Define group velocity window
- Exclude noise windows from processing
  - noise windows are selected to the first and last 1-min windows for RMT and only last 1-min window for UTTR from the selected processing window (red boxes, Fig. 5)
- Extract the points above the average of RMS amplitude powers (red circles)
- Extract continuous time points that exceed RMS amplitude threshold with durations of 5s or greater for RMT and 3s or greater for UTTR (blue dots)
- Signal duration defined by the continuous time that the signal threshold is exceeded (blue dots)
- Measure the SNR

Figure 5. Examples of RMT and UTTR waveforms with signal processing results (left) and automatic detections (blue) for RMT event (01/22/2009) recorded at 548 stations and UTTR event (08/01/2007) recorded at 451 stations with waveforms zoomed (right).

## Summary

- Automatic RMS amplitude measurements on seismic stations provides an initial detection threshold approach for infrasound signals, especially in combination with ground truth information.
- Such an approach provides an opportunity to investigate large data sets and assessment of the impact of noise characteristics.
- Implementation of this approach highlights the need to carefully assess both noise and signal characteristics.
- Preliminary results suggest the need for human review of detections in order to separate overlapping events.
- Application of these approaches provide a basis for investigation both time varying atmospheric effects as well as topographic effects on infrasound propagation.



Based on the analysis shown in this work, STA/LTA ratio (Trnkoczy, 1998) is applied for automatic detection in order to consider the background noise level. The above figure shows two examples of the detected signals (red) using STA/LTA ratio. LTA window,  $Tt$  (Trigger threshold),  $Dt$  (Detrigger threshold), PEM (pre-event time), and PET (post-event time) are automatically tuned with respect to signal characteristics and noise level. An additional 253 UTTR ground truth events will be tested using this method.